Multi-physical system identification to evaluate the transmission performance of a gearbox

Arash M. Zadeh Fard[1,2,*], Sven van Bree[1], Dennis Janssens[1,2], Matteo Kirchner[1,2], Koen Laurijssen[3], Niels Divens[3], Simon Vanpaemel[1,2], and Frank Naets[1,2]

[1]*Department of Mechanical Engineering, KU Leuven, Celestijnenlaan 300, Heverlee 3001, Belgium*
[2]*Flanders Make@KU Leuven, Belgium*
[3]*Flanders Make, Belgium*
[*]*arash.mohammadalizadehfard@kuleuven.be*

ABSTRACT

A coupled thermal and power loss model of a gearbox is developed to evaluate the efficiency. The setup is designed to investigate the dynamic performance and reliability of powertrains and consists of a permanent magnet motor, a drive motor, a gearbox, and a drive belt. Multiple sensors are installed to measure temperature, rotational speed, and torque in various tests. A combination of the least-squares method and extended Kalman filter exploits the model and measurements to estimate the parameters within the churning, meshing, and sealing power loss terms and the heat transfer coefficient, update the model, and make it setup-specific. The performance assessment of the identified model in experimental cases shows a good agreement between the predicted and measured temperature and power loss. The results show that the equivalent heat transfer coefficient significantly depends on the rotational speed and temperature.

INTRODUCTION

The efficiency of transmission systems is becoming increasingly important in a world moving towards a more sustainable future. As an essential part of a transmission system, predicting and optimizing the efficiency of a gearbox in the first step requires developing a representative thermo-mechanical power loss model. The power loss model should reflect the loss contributions of the existing components, including the gears, bearings, sealings, and auxiliary parts. Additionally, as the losses might depend on viscosity and hence temperature, a thermal model is required to update the temperature. Improving the efficiency can substantially affect power loss and operating temperature, contributing to better lubrication, less degradation, and reduced maintenance [1]. Many researchers have been focused on developing models to predict the mechanical performance of geared transmissions [2, 3, 4]. This research is part of an interdisciplinary project that aims to develop a digital twin for the entire power train by including the power electronics, electric motors, and gearbox to create a multi-disciplinary view of the system.

In this work, we develop and update a setup-specific multi-physical model for a gearbox. The power loss model considers the losses related to churning, meshing, rolling, sliding, drag, and sealing, and the belt and couples that with a lumped thermal model. The model's unknown parameters are estimated by performing several thermal and mechanical tests and applying the least-squares method and Extended Kalman Filter (EKF).

The gearbox is part of a setup designed to investigate the dynamic performance and reliability of electrified powertrains (Fig. 1). The setup consists of a permanent magnet motor, which functions as a drive motor to control the speed. This motor is linked to a two-stage Tramec gearbox (*ZA80B*), which, in turn, is connected to an induction motor through a belt to apply a predefined braking torque and emulate the road conditions. Several sensors are installed and connected to a dSPACE MicroLabBox to log temperature, torque, and rotational speeds. An HBM K-T40B sensor between the gearbox and motor measures the input torque. A telemetry torque sensor based on strain gauges is installed between the belt drive and the load motor to measure the output torque. Two pt100 sensors are used to measure the temperatures (sensors 1 and 2 in Fig. 1)

In the following section, the paper describes the power loss model. Afterward, the lumped thermal model is presented. The results section includes the performed tests and estimated parameters. The last

section provides the concluding remarks.

(a)
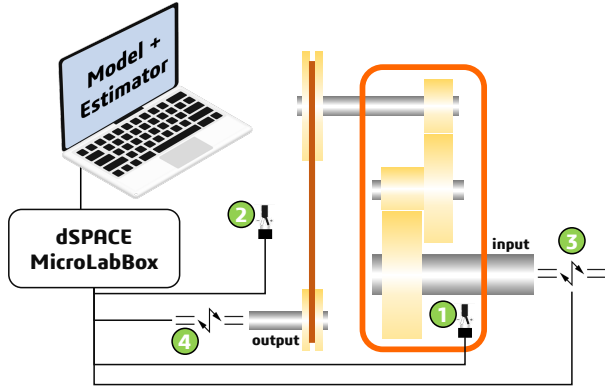
(b)

Figure 1: (a) Setup; (b) Installed sensors used in this study to measure (1) sump temperature, (2) ambient temperature, (3) input shaft's rotational speed and torque, and (4) output shaft's rotational speed and torque.

POWER LOSS MODEL

The efficiency of the gearbox and belt assembly can be defined as:

$$\eta = \frac{p_{out}}{p_{in}} = \frac{p_{in} - p_{loss}}{p_{in}} \qquad (1)$$

where p_{in}, p_{out}, and p_{loss} are the input power, output power, and power loss, respectively. The total power loss (p_{loss}) of a gearbox (Fig. 2) can be divided into load-dependent (p_l) and no-load losses (p_n) [5]:

$$p_{loss} = p_l + p_n. \qquad (2)$$

The terms in eq. (2) can be expressed as:

$$p_l = p_{mesh} + p_{bearing,l} + p_{belt}$$
$$p_n = p_{churn} + p_{bearing,n} + p_{seal}. \qquad (3)$$

In eq. (3), p_{mesh} and p_{churn} are load-dependent and load-independent loss terms related to the gears, respectively. This setup consists of two gear pairs as described in Table 1.

Table 1: Basic dimensions of the gears. Pinion 1 (p1) is on the input, wheel 1 (w1) and pinion 2 (p2) are on the intermediate, and wheel 2 (w2) is on the output shaft.

dimension	p1	w1	p2	w2
Z	20	51	12	48
module (mm)	1.75	1.75	2.5	2.5
β_b (°)	13.89	13.89	23	23

p_{mesh} is the load-dependent loss in the meshing zone of the gear pair [6]:

$$p_{mesh} = p_{in} H_\nu f \qquad (4)$$

where the gear loss factor (H_ν) is a function of the helix angle (β_b), number of teeth (Z_1 and Z_2), and transverse contact ratio (ϵ_α) [7]:

$$H_\nu = \frac{\pi}{cos(\beta_b)} \left(Z_1^{-1} + Z_2^{-1} \right) \left(1 - \epsilon_\alpha + \epsilon_1^2 + \epsilon_2^2 \right)$$
$$\epsilon_\alpha = \frac{g_f + g_a}{p_b} = \epsilon_1 + \epsilon_2. \qquad (5)$$

In eq. (5), g_f, g_a, and p_b are the length of approach, recess, and base pitch, respectively. Additionally, f in eq. (4) is the friction coefficient. In this research, the friction coefficient is calculated by updating Benedict and Kelley's empirical equation [8] for the current setup:

$$f = \alpha_1 \log_{10} \left(\frac{\alpha_2 F_{nu}}{\rho \nu V_g U^2} \right). \qquad (6)$$

In eq. (6) ρ, ν, V_g, U, and F_{nu} represent the lubricant density, kinematic viscosity, sliding velocity, sum of the rolling velocities, and normal load per unit length, respectively. Moreover, α_1 and α_2 are unknown parameters. Although this makes friction estimation relatively simple and accurate [7], it poses two drawbacks: first, at the pitch point, as the relative motion of the two meshing gears is of pure rolling nature, the sliding velocity is zero, and the friction coefficient becomes infinite [7]; Second, eq. (4) is only applicable if the friction coefficient is constant over the entire contact line [5]. Therefore, the average friction coefficient is used in this paper.

To reduce friction and wear in the contacts of the gears and bearings, the gearbox sump is filled partially with *Gear-OM320* lubricating oil from Ardeca. p_{churn} arises due to gear movement in the partial oil immersion conditions [6]:

$$p_{churn} = \frac{1}{16} C_m \rho \omega^3 S_m d_p^3 \qquad (7)$$

where C_m, ω, S_m, and d_p are the dimensionless drag torque coefficient, rotational speed, the submerged surface area of the rotating gear, and the pitch diameter, respectively.

Changenet et al. [7] determined C_m by doing a dimensional analysis and considering the effect of geometrical parameters related to the gear and oil sump, oil characteristics, and rotational speed:

$$C_m = \beta_1 \left(\frac{b}{d_p}\right)^{\beta_2} \left(\frac{h}{d_p}\right)^{\beta_3} \left(\frac{V_0}{d_p^3}\right)^{\beta_4} Re^{\beta_5} Fr^{\beta_6}. \quad (8)$$

In eq. (12), b, h, and V_0 are the face width of the gear, submerged depth of the gear, and oil volume, respectively. Additionally, Re and Fr are the Reynolds and Froude numbers, and β_1 to β_6 are model parameters. Changenet et al. [7] have determined the model parameters by performing various experiments with different oils, oil heights, gears, and speeds. This paper uses the same exponents (β_2 to β_6) but updates β_1 as updating all of them requires a lot of tests at various conditions (e.g., at different face widths and oil levels).

The setup uses six single-row tapered roller bearings (32004X, 30302, 30204, and 32010X). The load-dependent and load-independent losses in the bearings are divided into rolling ($p_{rolling}$), sliding ($p_{sliding}$), and drag (p_{drag}) contributions:

$$p_{bearing} = p_{rolling} + p_{sliding} + p_{drag}. \quad (9)$$

All the bearing-related loss components were calculated using the empirical equations and tables provided by Harris et al. and SKF [9, 10].

The belt-pulley-related power loss (p_{belt}) in eq. (3) is modeled with a viscous friction model. Finally, the seal-related power loss (p_{seal}) is considered an unknown constant and determined based on the performed measurements.

As the power loss occurs, the oil temperature and viscosity change (Fig. 2). This paper uses Andrade's correlation to describe how temperature and viscosity are related:

$$\nu = c_1 exp(\frac{c_2}{\bar{\theta}}) \quad (10)$$

where $\bar{\theta} = \theta + 273.15$ is the absolute temperature. The constants c_1 and c_2 are calculated by inserting the known viscosity at $\theta = 40 \ {}^oC$ and $\theta = 100 \ {}^oC$.

This paper updates α_1, β_1, and p_{seal} based on the performed experiments using the least squares method. According to eq. (3), eq. (6), and eq. (12), α_1 is related to the load-dependent losses, while β_1 and p_{seal} are present in load-independent power loss terms. The belt was first disconnected, and a set of experiments were performed at different rotational speeds to update the load-independent terms (β_1 and p_{seal}). Afterward, the belt was connected, and a second set of experiments was conducted at different torque (load) levels to update the load-dependent terms.
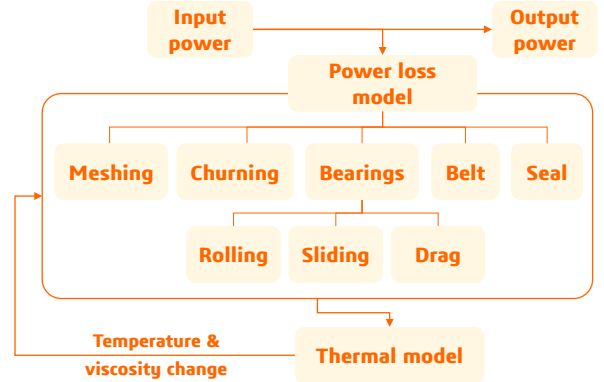
Figure 2: Coupled thermal and power loss models.

THERMAL MODEL

A lumped parameter thermal model is used to predict the temperature and update viscosity:

$$mc_{p,eq}\Delta\dot{\theta}_{sump}(t) = -\hbar A_{eq}(\theta,\omega)\Delta\theta_{sump} + p_{loss} \quad (11)$$

where $mc_{p,eq}$ is the equivalent heat capacity, including the gears, bearings, shafts, and oil. Additionally, $\Delta\theta_{sump} = \theta_{sump} - \theta_\infty$ and $\hbar A_{eq}$ are the temperature difference between the sump and ambient and the equivalent heat transfer coefficient, respectively. An augmented Extended Kalman Filter (EKF) [11] is applied to estimate the heat transfer coefficient's profile using the random walk model [12, 13]:

$$\hbar\dot{A}_{eq} = 0 + w_{\hbar A_{eq}} \quad (12)$$

where $w_{\hbar A_{eq}} \sim \mathcal{N}(0, Q_{\hbar A})$ is Gaussian noise input with zero mean. Experiments were performed at different working conditions to estimate $\hbar A_{eq}$ as the heat transfer coefficient can be a function of temperature and rotational speed.

RESULTS

Several tests are performed to estimate the unknown parameters in the power loss and thermal model (α_1, β_1, p_{seal}, and $\hbar A_{eq}$) and update the model for the existing setup as summarized in Table 2. Table 3 includes the known parameters.

Table 2: Performed tests.

test	belt	ω_{in} [rpm]	T_{in} [N.m]
1	disconnected	500 to 3000	-
2	connected	460	10 to 30
3	connected	1000	10
4	connected	3000	10
5	connected	5000	10

Table 3: Known parameters.

parameter	value
ρ	0.9 kg.l^{-1}
ν_{40^oC}	330 mm^2.s^{-1}
ν_{100^oC}	24.2 mm^2.s^{-1}
α_2	291205.8×10^{-6}
β_2	0
β_3	0.45
β_4	0.1
β_5	-0.21
β_6	-0.6

Churning and sealing power losses are load-independent, so the belt is disconnected in the first set of experiments (Table 2, test 1). To capture the speed-dependent behavior, the rotational speed is changed from 500 rpm to 3000 rpm (in steps of 250 rpm) in this test set (Fig. 3 a). The least squares method updates β_1 in eq. (12) and p_{seal} in eq. (3). Comparing the measured and model-predicted power losses presented in Fig. 3 b shows an accuracy of 97.87 % for the unloaded gearbox (belt disconnected).

(a)

(b)
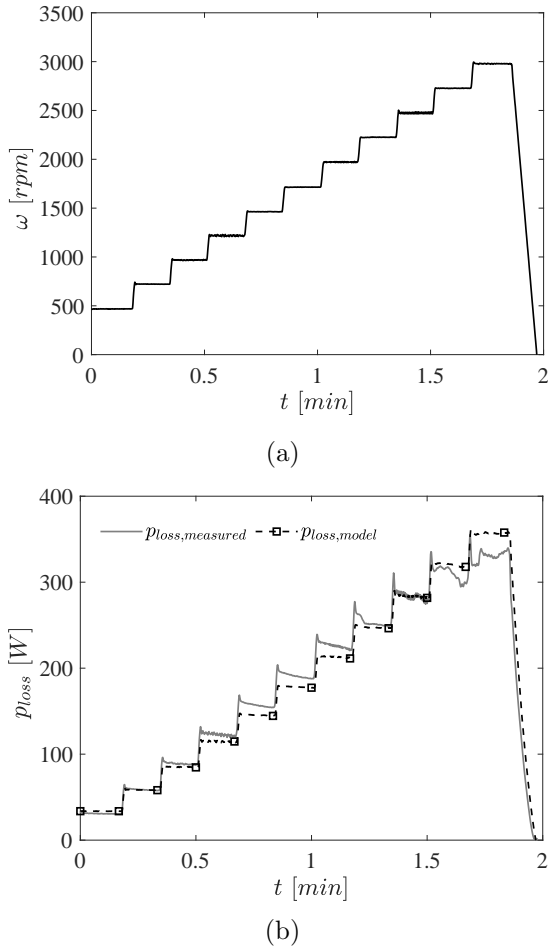
Figure 3: Belt disconnected; (a) rotational speed, (b) predicted and measured power loss.

In the next step, the measurements in the second set of tests (Table 2, test 2) are used to update the load-dependent meshing loss (α_1 in eq. (6)). In this set, the rotational speed is kept constant while torque changes from 10 N.m to 30 N.m (Fig. 4 a). For the loaded gearbox, comparing the measured and predicted power losses (Fig. 4 b) shows an accuracy of 95.61 % (belt connected). Based on the results, the power loss is influenced by load and rotational speed.

(a)

(b)
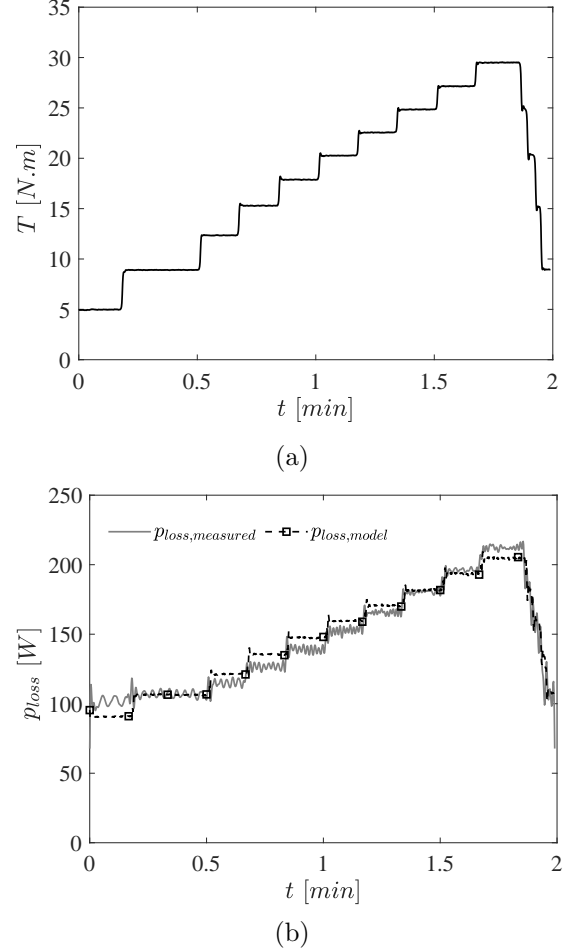
Figure 4: Belt connected; (a) torque, (b) predicted and measured power loss.

A set of other experiments are performed and used to estimate the equivalent heat transfer coefficient for the gearbox (Table 2, tests 3, 4, and 5). In each test, the set torque and rotational speeds are kept constant. The temperature, rotational speeds, and torques are logged for these tests until the sump reaches a steady temperature. Afterward, a low-pass filter is used to pre-process the measurements. Next, an EKF exploits the model and measurements to estimate the heat transfer coefficient.

Fig. 5 and Fig. 6 show the measured temperatures and power loss along with the estimated $\hbar A_{eq}$ for $\omega = 1000$ rpm and $\omega = 5000$ rpm, respectively. Comparing the temperature difference ($\Delta\theta_{sump}$) on both

figures shows that by increasing the rotational speed from 1000 rpm to 5000 rpm, the gearbox steady temperature increases from 11.5 ^oC to 29.2 ^oC. Additionally, the power loss has a significant increase (from 0.25 kW for $\omega = 1000$ rpm to 1.20 kW for $\omega = 5000$ rpm in the steady part of the temperature profile). Besides, due to the temperature rise, the power loss constantly decreases throughout the experiment.
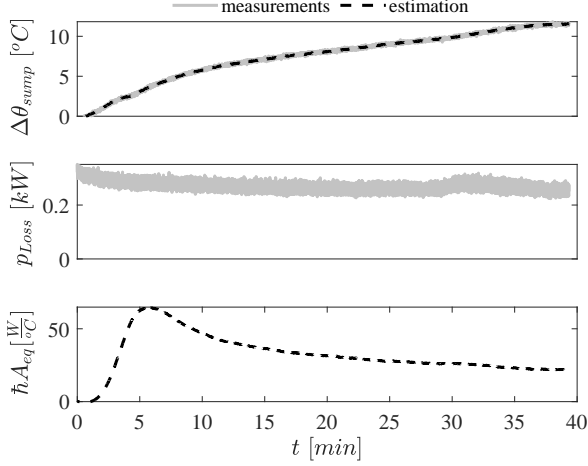
Figure 5: Heat transfer coefficient at ω=1000 rpm.
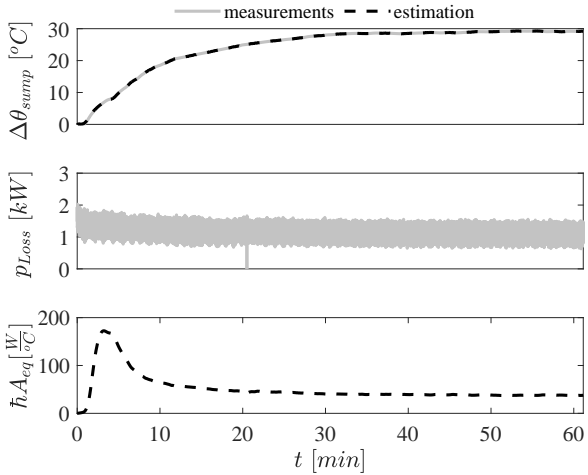
Figure 6: Heat transfer coefficient at ω=5000 rpm.

The estimated heat transfer coefficients at different conditions are used to fit a surface for $\hbar A_{eq}$ at different rotational speeds and temperatures using a piecewise linear function (Fig. 7). As shown in Fig. 7, $\hbar A_{eq}$ experiences a peak for a constant rotational speed. Although the heat transfer coefficient can be a function of rotational speed and temperature [14, 15, 16], the variation, in this case, might be partially due to the one-lumped mass assumption for the thermal model.
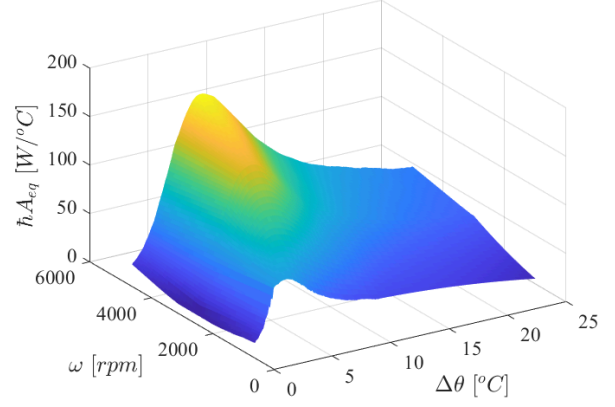
Figure 7: Equivalent heat transfer coefficient.

The updated model is used in an experimental case to predict the power loss and temperature profile. As shown in Fig. 8, the model underestimates the power loss.
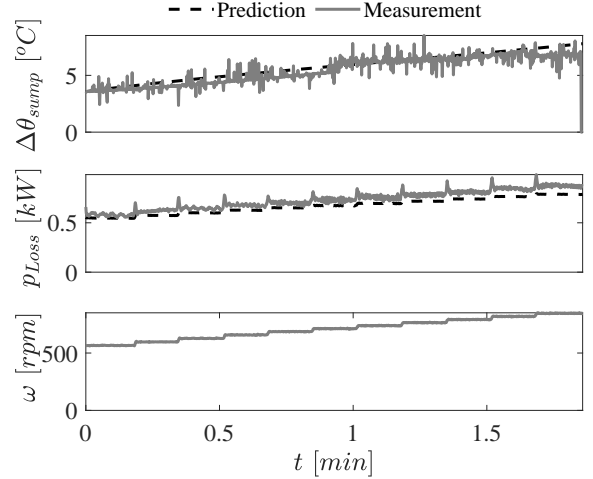
Figure 8: Predicted and measured temperature and power loss in an experimental case.

CONCLUSION AND DISCUSSION

A coupled thermal and power loss model is developed for a gearbox. A combination of the least-squares method and EKF exploits the model and measurements to estimate the model unknowns. The results show that the heat transfer coefficient depends on the rotational speed. The performance assessment of the identified model in an experimental case shows a good agreement between the predicted and measured temperature and power loss. The developed model will be coupled with the models of the power electronics and drive motor to evaluate the system-level performance of the drive train.

ACKNOWLEDGMENTS

REFERENCES

[1] C. M. Fernandes, P. M. Marques, R. C. Martins, and J. H. Seabra, "Gearbox power loss. part i: Losses in rolling bearings," *Tribology International*, vol. 88, pp. 298–308, 2015.

[2] M. N. Mastrone, E. A. Hartono, V. Chernoray, and F. Concli, "Oil distribution and churning losses of gearboxes: Experimental and numerical analysis," *Tribology International*, vol. 151, p. 106496, 2020.

[3] H. R. F. Fotso, C. V. A. Kazé, and G. D. Kenmoé, "Real-time rolling bearing power loss in wind turbine gearbox modeling and prediction based on calculations and artificial neural network," *Tribology International*, vol. 163, p. 107171, 2021.

[4] P. M. Marques, R. C. Martins, and J. H. Seabra, "Power loss and load distribution models including frictional effects for spur and helical gears," *Mechanism and Machine Theory*, vol. 96, pp. 1–25, 2016.

[5] C. M. Fernandes, P. M. Marques, R. C. Martins, and J. H. Seabra, "Gearbox power loss. part ii: Friction losses in gears," *Tribology International*, vol. 88, pp. 309–316, 2015.

[6] B. Zhu, X. Wang, L. Luo, N. Zhang, and X. Liu, "Influence of lubricant supply on thermal and efficient performances of a gear reducer for electric vehicles," *Journal of Tribology*, vol. 144, no. 1, 2022.

[7] C. Changenet, X. Oviedo-Marlot, and P. Velex, "Power loss predictions in geared transmissions using thermal networks-applications to a six-speed manual gearbox," 2006.

[8] G. Benedict and B. Kelley, "Instantaneous coefficients of gear tooth friction," *ASLE transactions*, vol. 4, no. 1, pp. 59–70, 1961.

[9] T. A. Harris and M. N. Kotzalas, *Essential concepts of bearing technology.* CRC press, 2006.

[10] S. Group *et al.*, "Skf general catalogue," *SKF Group*, 2008.

[11] F. Naets, J. Croes, and W. Desmet, "An online coupled state/input/parameter estimation approach for structural dynamics," *Computer Methods in Applied Mechanics and Engineering*, vol. 283, pp. 1167–1188, 2015.

[12] A. M. Zadeh Fard, F. A. Garcia, M. Kirchner, B. Blockmans, W. Desmet, and F. Naets, "Comparing the ekf with inverse black-box models in system identification of a chemical stirred tank," in *2023 International Conference on Control, Automation and Diagnosis (ICCAD)*, pp. 1–6, IEEE, 2023.

[13] A. M. Zadeh Fard, M. Kirchner, W. Arts, *et al.*, "Nonlinear multi-physical system identification of a chemical stirred tank," in *22nd IFAC World Congress*, Elsevier Ltd, 2023.

[14] R. Caillaud, C. Buttay, R. Mrad, J. Le Lesle, F. Morel, N. Degrenne, and S. V. Mollov, "Thermal considerations of a power converter with components embedded in printed circuit boards," *IEEE Transactions on Components, Packaging and Manufacturing Technology*, vol. 10, no. 2, pp. 230–239, 2019.

[15] M. Hnizdil, M. Chabicovsky, M. Raudensky, and T.-W. Lee, "Heat transfer during spray cooling of flat surfaces with water at large reynolds numbers," *Journal of Flow Control, Measurement & Visualization*, vol. 4, no. 3, pp. 104–113, 2016.

[16] P. Shams Ghahfarokhi, A. Kallaste, A. Podgornovs, A. Belahcen, T. Vaimann, and B. Asad, "Determination of heat transfer coefficient of finned housing of a tefc variable speed motor," *Electrical Engineering*, vol. 103, pp. 1009–1017, 2021.